Dispersion-Based Fresh-Slice Scheme for Free-Electron Lasers

Marc W. Guetg, Alberto A. Lutman, Yuantao Ding, Timothy J. Maxwell, and Zhirong Huang

Phys. Rev. Lett. **120**, 264802 — Published 28 June 2018

DOI: 10.1103/PhysRevLett.120.264802

Dispersion-based Fresh-slice Scheme for Free-Electron Lasers

Marc W Guetg,* Alberto A Lutman, Yuantao Ding, Timothy J Maxwell, and Zhirong Huang
SLAC National Accelerator Laboratory, Menlo Park, California 94025, USA

The Fresh-slice technique improved the performance of several Self-Amplified Spontaneous Emission Free-Electron laser schemes by granting selective control on the temporal lasing slice without spoiling the other electron bunch slices. So far, the implementation required a special insertion device to create the beam yaw, called dechirper. We demonstrate a novel scheme to enable Fresh-slice operation based on electron energy chirp and orbit dispersion that can be implemented at any free-electron laser facility without additional hardware.

X-ray free-electrons lasers (XFEL) are the brightest X-ray light sources for scientific applications [1, 2]. With their high-intensity photon pulses, XFELs have been used in a broad range of scientific experiments in the physical [3], chemical [4], life [5] and material sciences [6]. X-ray FEL machines were initially designed to produce a single X-ray pulse with a duration ranging from tens to hundreds of femtoseconds. Recently, in an effort to satisfy the requirements of the wide scientific community, FEL X-ray shaping has been an active field of investigation. Ultra-short pulses are produced to exploit the probe before destroy principle for single-particle imaging [7, 8] and femtosecond X-ray crystallography [9] with an array of techniques [10–15]. Few femtoseconds intense pulses can be produced with multi-stage Fresh-slice amplification [16] and are suitable for creating double core-hole states [17] and to reveal a variety of non-linear phenomena when intense X-ray pulses interact with atoms and molecules [3, 18], including stimulated emission [19]. X-ray pump, X-ray probe experiments (see for example [20, 21]) were enabled by double-pulse schemes [22–26]. Narrow bandwidth and spectral stability granted by the self-seeding schemes [27, 28] were used to study the dynamics of warm dense matter system [29] and for X-ray absorption spectroscopy [30].

The recent demonstration of the Fresh-slice [26] technique enabled or improved the performance of many aforementioned schemes. The Fresh-slice scheme grants control over the temporal slice lasing in each undulator section by manipulating the orbits of individual slices. A device imparts a time-dependent kick to the electrons causing the bunch slices to travel on monotonically increasing oscillating trajectories in the strong focusing lattice. In an undulator section, the sustained coherent interaction between a microbunched beam and the electromagnetic field is not preserved for a large oscillatory orbit[10, 31], and therefore the lasing slice can be selected as the one travelling on a straight orbit.

Unlike other techniques [11–13], the lasing-suppressed slices retain full lasing capability to be exploited in downstream undulator sections. In two-color modes higher power and enhanced pulse customizability were demonstrated. Three fully saturated X-ray pulses of different colors were produced for the first time. High power single-coherent spikes were demonstrated in a multi-stage scheme [16], and by using additional cascaded amplification stages terawatt powers could be reached [32]. Combined with self-seeding, the Fresh-slice technique improved the achievable power in the hard X-rays [33]. It is planned to be used for harmonic lasing at the LCLS [34] and to produce double sub-femtosecond pulses [35].

The Fresh-slice technique has been demonstrated by tailoring the electron bunch with a temporal-transverse correlation and subsequent fine bunch orbit control in the undulator line. Alternatively, a scheme based on time-dependent matching rather than orbit has been proposed [36, 37], which exploits the transverse focusing term of the dechirper [37]. At the LCLS the temporal-transverse correlation is imparted by the strong transverse wakefield of a dechirper [38–40] providing sufficient beam yaw for the lasing suppression. Alternatively, a quadrupole magnet in a dispersive area and transverse deflecting cavities were also proposed to induce the required beam yaw [31, 41, 42].

This Letter describes the first demonstration of a Fresh-slice scheme based on electron energy chirp and orbit dispersion. In contrast to other Fresh-slice implementations, the presented one does not require any special insertion device and therefore can be used at any existing XFEL facility without the installation of additional hardware. Dispersion-based Fresh-slice represents a viable solution for future high-repetition rate machines where dechirper based schemes may suffer from the violation of beam stay clear requirements [43] and excessive heating on the dechirper jaws. Furthermore, provided a linearly energy chirped electron bunch in the dispersive area, the induced beam yaw is linear granting more uniform pulse durations in double-pulse modes. This pulse length uniformity is important for non-linear two-photon-two-color interactions as the shorter pulse limits the overlap. Furthermore, the longer pulse limits the temporal resolution for any x-ray pump y-ray probe and x-ray probe x-ray probe experiments therefore making it more suited for this experiments than the dechirper based Fresh-slice scheme.

Similar to the dechirper-based method, the dispersion one does not suffer from beam arrival time to radio-frequency phase jitter, which is a limitation of the

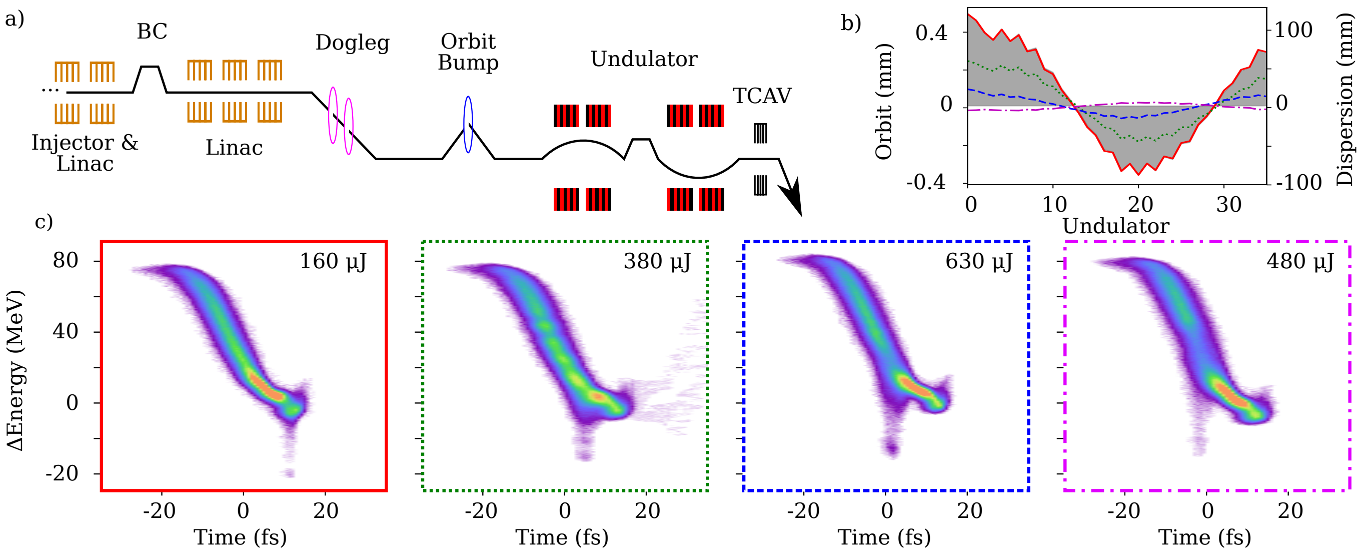

FIG. 1. a) Schematic experimental setup for the LCLS. The electrons coming from the linac (left) are over-compressed in the last bunch compressor, followed by the last linac section adding both energy and chirp, which is followed by the dogleg, containing two tweaker quadrupole magnets (magenta) to control dispersion, followed by an orbit bump (blue) and the undulators (red/black). A transverse deflector following spectrometer allows direct longitudinal phase space measurements. b): Dispersion (filled, gray) within the undulator with 4 different selected orbits leading to selective lasing within the electron beams shown in c). Electron beam energy: 10.1 GeV, charge: 185 pC.

radio-frequency transverse deflecting cavity implementation. Finally, the presented scheme stabilizes FEL radiation wavelength granting an advantage over competing schemes when generating a single short pulse from a long electron bunch. This could lead to an improved usage of stochastic stimulated x-ray Raman spectroscopy [44] and easier data sorting for serial fs crystallography [45]. Furthermore, the energy stabilization could also lead to improved Fresh-slice self-seeding performance as the bandwidth stability is believed to be one of the limiting factors.

In the dispersion based Fresh-slice scheme presented here, the beam yaw required to select lasing slices is created by controlling the dispersion in a beam with large energy chirp. Fig. 1.a illustrates a schematic drawing of the LCLS with parts relevant to the demonstrated scheme. The electron bunch is accelerated in the linac sections (orange) and compressed in two bunch compressors (BCs). Over-compressing the electron bunch within the last BC flip the sign of the energy chirp. The longitudinal wakefields of the third section of the linac further increase the energy chirp when operating in over-compression mode, allowing to generate energy chirps well above 1%, the size commonly used for large-bandwidth lasing. The over-compressed bunch then traverses a dispersive dogleg section with two dispersion tweaker quadrupoles to manipulate the dispersion. In a dispersive section, particles with different longitudinal momentum travel on different transverse orbits. When passing the quadrupoles, the electrons receive a transverse kick depending on their transverse trajectory. For an electron bunch with an energy chirp traveling through a dispersive section this is a mean to introduce a time dependent kick, which then translates into a beam yaw through betatronic phase advance. The amount of beam yaw can be controlled by increasing either the energy chirp or dispersion.

LCLS is equipped with a pair of quadrupole magnets to finely control dispersion in amplitude and phase in both bunch compressors and the final dogleg. Alternatively, the dispersion was controlled by orbit bumps after the final dogleg. Hereby the dispersion was manipulated by introduction of an orbit offset within strong quadrupole magnets. This method has the added benefit of not altering transverse matching and therefore not requiring rematching.

Finally, the bunch enters the undulator line, which is split in three sections separated by magnetic chicanes introduced for self-seeding schemes [27, 28, 46]. In addition, there is a pair of orthogonal orbit correctors between each undulator segment to control the orbit position and angle. Only electrons traveling on axis through the undulator contribute to lasing, so selection of the lasing slice is done by setting a proper electron bunch orbit in the undulator line (Fig. 1.b). Steering the orbit within the undulator line enables selection of different lasing slices for different sections (Fig. 1.c).

Since different slices have different electron energies, they lase at different colors, so two-color double pulses with a wide range of color separation can be produced by changing the orbit between undulator sections. The time difference between the photon pulses is mainly controlled by a magnetic chicane located between the undulator sections, which delays the arrival of the lasing electron slice in the downstream undulator section with respect to the upstream generated photon pulse (See also Fig. 4.a). When a slice on the bunch tail is used to produce the X-ray pulse in the upstream undulator section, then the delay between the pulses can be scanned smoothly through the time coincidence. Instead, if the pulse produced in the upstream undulator section is on the bunch head there is a minimum delay of ten to few tens of femtoseconds between the two pulses. Thus, if pulse overlap, or scanning in the first few femtoseconds delay range is required for an experiment, then the possible photon energy range at LCLS is asymmetric, with the pulse produced from the bunch tail (pump) ranging from the same wavelength to -4% compared to the pulse produced from the bunch head (probe).

Inherent to the dispersion based Fresh-slice scheme is a stable FEL radiation wavelength, which is not affected by the electron bunch energy jitter as long as the jitter is smaller than the unsuppressed FEL bandwidth, which is normally given. For this specific experiment by more than one order of magnitude. For a SASE FEL, the radiated photon energy is proportional to the square of the electron energy, leading to a relative photon energy jitter twice the relative electron energy jitter. Using the dispersion based Fresh-slice scheme, the lasing slice is selected as the one traveling on a straight line in the undulator line, which corresponds to an electron bunch slice with defined energy. Therefore, the electron bunch shot-to-shot energy jitter causes a jitter in the position of the lasing slice instead of a radiation wavelength jitter. This is a valuable feature unique to the presented method. For instance, in the dechirper-based Fresh-slice the lasing slice is selected as a bunch slice having a defined temporal coordinate within the bunch [26] and the lasing wavelength is thus sensitive to electron energy jitter. For a slotted-foil pulse duration control scheme [12], energy selection occurs in the second bunch compressor, but energy jitter can still be added in the third linac section and thus influence radiation wavelength.

The demonstration of selective lasing control was performed at the LCLS in over-compression mode for several energies. The electron bunch was operated at nominal charge of 250 pC at the injector and collimated to 180 pC at the first bunch compressor [47]. For soft x-rays, the electron bunch energy was 5680 ± 3.1 (rms) MeV and a photon energy jitter of 0.08% was measured.

For the experiments presented in this Letter, the undulator orbit was set by manipulating multiple correctors in the undulator line, and just upstream from the undulator line. The target orbit was chosen by scaling the orbit recorded after a perturbation of the tweaker quadrupole magnet with the transverse orbit feedbacks turned off. The amount of scaling required for lasing on a particular slice was determined empirically by observing the lasing

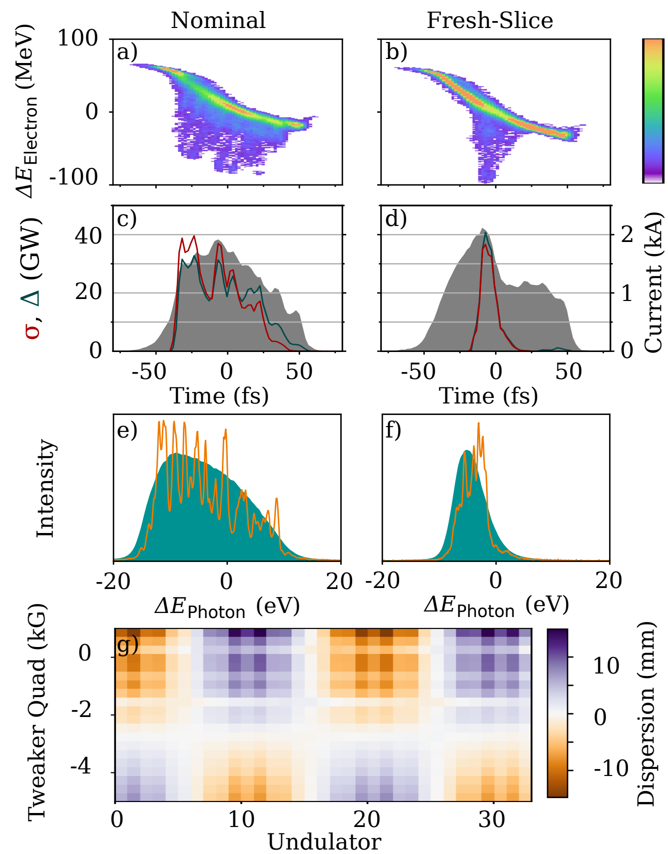

FIG. 2. Left: Uniform lasing. Right: Fresh-slice lasing. a, b) Longitudinal electron phase space after the undulator. c, d): Photon power calculated by energy loss (Δ, green) and slice energy spread (σ, red) overlaid over the current profile (grey). e, f) Single shot (brown) and average (cyan) photon spectrum. g) Dispersion within the undulator created by scanning the second tweaker quadrupole magnet within the dog leg. Electron charge 180 pC, electron energy 5.68 GeV, mean photon energy 1.5 keV.

footprint of the time-resolved electron bunch phase space downstream of the undulator line.

Comparing the time-resolved electron bunch energy spaces downstream of the undulator line (Fig. 2(a,b)) reveals that both setups have the same amount of electron energy loss, which indicates that FEL power was not altered by the Fresh-slice scheme. The X-ray power temporal profile (Fig. 2(c,d)) was measured by analyzing the time-resolved electron phase-space lasing-on footprints compared to the lasing-off ones [48]. The FEL process increases both the slice energy spread and decreases the slice centroid energy. The temporal profile of the photon pulse was estimated independently with both of the quantities.

The measurement based on the energy spread increase in red agrees well with the one based on the slice energy losses in blue. These measurements show how the X-ray pulse duration is reduced through the Fresh-slice scheme. Comparing single-shot or average spectra for each setup

(Fig. 2(e,f)) as measured at the soft X-ray experimental station with a grating spectrometer [49, 50] shows that the Fresh-slice scheme also narrows the spectral width of the X-ray pulse. Fig. 2.g shows the dispersion within the undulator by scanning a tweaker quadrupole within the dogleg. Together with the energy chirp this is a measurement of the off-axis oscillation amplitude of individual slices.

To further investigate the spectral stability of the scheme, we compared the setup in standard over-compression mode (low dispersion) to Fresh-slice mode (high dispersion). Fig. 3(a) displays the ratio between photon energy jitter and electron bunch energy jitter as function of the dispersion in Genesis [51] simulations and measurements. It shows that for large absolute dispersion values, corresponding to Fresh-slice mode, the photon wavelength is stable while there is no wavelength stabilization for low dispersion values. Next, two experimental operating points were considered, one with minimal dispersion and one with large dispersion (Fig. 3(b)). Comparing the average photon spectra as function of electron bunch energy shows a stable wavelength and narrow bandwidth for large dispersion, while at low dispersion the wavelength is energy dependent and spectral bandwidth is wide.

Looking at the electron orbit position within the undulator line for shots at higher or lower than target electron energy (Fig. 3.e) we observe that the orbit shifts in high dispersion mode while it remains constant for the low dispersion mode. This orbit shift inherent to the Fresh-slice mode results in selection of a different lasing slice and thereby corrects for the offset in electron bunch energy, leading to the observed spectral stability.

To further explore the capabilities of the method, a two-color scheme with dispersion-based Fresh-slice was developed. A first color was produced on the bunch core in the first undulator section, before the second chicane of the LCLS undulator line. Downstream of the chicane the orbit was manipulated to lase on a slice toward the bunch tail. We repeated the experiment for two different slices on the bunch tail while keeping the first color constant. Fig. 4.a shows the position of the bunch orbit center of mass throughout the undulator. In the first undulator section, the lasing slice is on the bunch core, so the orbit does not oscillate, while in the second undulator section the lasing slice is distant from the bunch core which is visible by the oscillation of the orbit. Selecting a lasing slice closer to the bunch core (green) requires an orbit with lower oscillation amplitude while a lasing slice more distant to the core (red) needs higher amplitude. Using the slice closer to the bunch core (blue) resulted in an energy separation between the two colors of $\sim$ 30 eV (Fig. 4.b green) while using the slice more distant to the core (red) produced X-rays with a separation of $\sim$ 60 eV. This corresponds to a relative energy separation of 4%, which is the widest relative color separation of photon

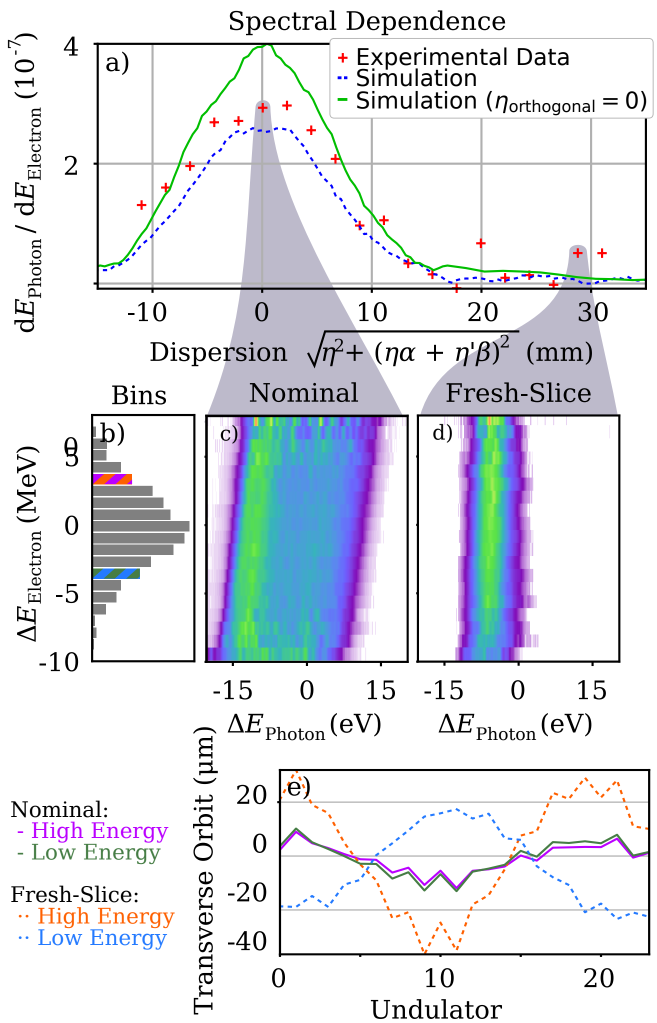

FIG. 3. a) Spectral stability of the photon beam for measurement (red), genesis [51] simulation of it (blue) and an idealized case (green) without dispersion in the orthogonal to the measurement plane. c, d) Spectral measurements of two dispersion settings (marked grey area). The spectra are averaged and binned by electron energy. b) Histogram showing the energy distribution of the measured pulses. e) The averaged electron orbits for both one high and low energy bin (marked in histogram middle/left). For the low dispersion case both orbits are on top of each other. Electron Energy: 5.68 GeV, photon energy: 1.5 keV. Electron beam was kicked after undulator 25 to preserve suppression.

pulses at LCLS observed in any two-color mode so far.

The temporal delay between the photon pulses initially depends on the temporal distance between the selected lasing slices and slippage, but it can be adjusted by a time delay introduced at the magnetic chicane located between undulator sections. Therefore, the temporal delay between pulses is virtually independent of the chosen pulse colors.

In machines with variable gap undulators each pulse wavelength can be independently adjusted in a wide range by the strength K of the undulators[23]. How-

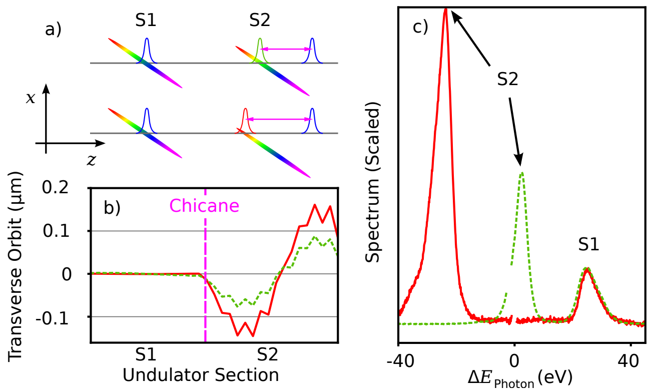

FIG. 4. a) Schematic drawing of two color operation with lasing in two locations of the same electron bunch. b) shows two measured electron orbits selecting a common first color and a individual second. The delay between the pulses is controlled by a self seeding chicane (magenta). c) Average spectrum of both cases. The missing spectral data is due to broken YAG scintillator. Mean photon energy: 1.5 keV. With individual shots of over 100 µJ (average 20 µJ) with a color separation of more than 4%

ever the LCLS K range is already sufficient to tune the different slices at the same wavelength, thereby enabling the multi-stage amplification schemes [16]. Controlling the dispersion within the second bunch compressor is an alternative method to produce a tilted beam without using the over-compression mode or additional hardware. However, transporting such beam from the bunch compressor to the undulator line can degrade the electron bunch quality for slices travelling off-axis, and the energy stabilization would no longer be superior to the one provided by the slotted foil. In summary, we demonstrated a dispersion-based Fresh-slice scheme readily available at any XFEL facility without additional hardware. Control of the required dispersion, energy chirp and orbit are simple to be implemented and the scheme offers improved spectral stability. The latter feature is valuable for experiments requiring wavelength stability in a short pulse and multi-stage self-seeding schemes [33].

This work has been supported by DOE contract #DE-AC02-76SF00515. The authors thank the operators of LCLS for their excellent handling of the machine and Sandra Guetg for proofreading the manuscript. Furthermore, the authors thank Uwe Bergmann for fruitfull discussions.

* marcg@slac.stanford.edu

[1] P. Emma *et al.*, Nature Photonics **4**, 641 (2010).
[2] T. Ishikawa *et al.*, Nat. Photon. **6**, 540 (2012).
[3] Young *et al.*, Nature **466**, 56 (2010).
[4] W. Zhang *et al.*, Nature **509**, 345 EP (2014).
[5] H. N. Chapman *et al.*, Nature **470**, 78 (2011).
[6] D. Milathianaki *et al.*, Science **342**, 220 (2013), http://science.sciencemag.org/content/342/6155/220.full.pdf.
[7] M. Seibert *et al.*, Nature **470**, 73 (2011).
[8] A. Aquila *et al.*, Structural Dynamics **2**, 041701 (2015), https://doi.org/10.1063/1.4918726.
[9] H. N. Chapman, C. Caleman, and N. Timneanu, Philosophical Transactions of the Royal Society of London B: Biological Sciences **369** (2014), 10.1098/rstb.2013.0313.
[10] M. W. Guetg, A. A. Lutman, Y. Ding, T. J. Maxwell, F.-J. Decker, U. Bergmann, and Z. Huang, Phys. Rev. Lett. **120**, 014801 (2018).
[11] P. Emma, K. Bane, M. Cornacchia, Z. Huang, H. Schlarb, G. Stupakov, and D. Walz, Phys. Rev. Lett. **92**, 074801 (2004).
[12] Y. Ding *et al.*, Applied Physics Letters **107**, 191104 (2015), 10.1063/1.4935429.
[13] A. Marinelli, R. Coffee, S. Vetter, P. Hering, G. N. West, S. Gilevich, A. A. Lutman, S. Li, T. Maxwell, J. Galayda, A. Fry, and Z. Huang, Phys. Rev. Lett. **116**, 254801 (2016).
[14] S. Huang, Y. Ding, Y. Feng, E. Hemsing, Z. Huang, J. Krzywinski, A. A. Lutman, A. Marinelli, T. J. Maxwell, and D. Zhu, Phys. Rev. Lett. **119**, 154801 (2017).
[15] A. Marinelli, J. MacArthur, P. Emma, M. Guetg, C. Field, D. Kharakh, A. A. Lutman, Y. Ding, and Z. Huang, Applied Physics Letters **111**, 151101 (2017), https://doi.org/10.1063/1.4990716.
[16] A. A. Lutman, M. Guetg, T. J. Maxwell, J. P. M. Y. Ding, C. Emma, J. Krzywinski, and A. Marinelli, Phys. Rev. Lett. (2018), submitted.
[17] N. Berrah *et al.*, Proceedings of the National Academy of Sciences **108**, 16912 (2011), http://www.pnas.org/content/108/41/16912.full.pdf.
[18] J. Stöhr and A. Scherz, Phys. Rev. Lett. **115**, 107402 (2015).
[19] T. Kroll *et al.*, Phys. Rev. Lett. **120**, 133203 (2018).
[20] K. R. Ferguson *et al.*, Science Advances **2** (2016), 10.1126/sciadv.1500837.
[21] A. Picón *et al.*, Nature Communications **7**, 11652 EP (2016), article.
[22] A. A. Lutman, R. Coffee, Y. Ding, Z. Huang, J. Krzywinski, T. Maxwell, M. Messerschmidt, and H.-D. Nuhn, Phys. Rev. Lett. **110**, 134801 (2013).
[23] T. Hara *et al.*, Nature Communications **4**, 2919 (2013).
[24] A. Marinelli, A. A. Lutman, J. Wu, Y. Ding, J. Krzywinski, H.-D. Nuhn, Y. Feng, R. N. Coffee, and C. Pellegrini, Phys. Rev. Lett. **111**, 134801 (2013).
[25] A. Marinelli *et al.*, Nature Communications **6** (2015), 10.1038/ncomms6369.
[26] A. A. Lutman, T. J. Maxwell, J. P. MacArthur, M. W. Guetg, N. Berrah, R. N. Coffee, Y. Ding, Z. Huang, A. Marinelli, S. Moeller, and J. C. U. Zemella, Nat Photon **10**, 745 (2016).
[27] A. A. Lutman *et al.*, Phys. Rev. Lett. **113**, 254801 (2014).
[28] D. Ratner *et al.*, Phys. Rev. Lett. **114**, 054801 (2015).
[29] L. B. Fletcher *et al.*, Nature Photonics **9**, 274 EP (2015), article.
[30] T. Kroll *et al.*, Opt. Express **24**, 22469 (2016).
[31] M. W. Guetg, B. Beutner, and E. P. S. Reiche, Phys. Rev. ST Accel. Beams **18**, 030701 (2015).
[32] E. Prat, F. Löhl, and S. Reiche, Phys. Rev. ST Accel. Beams **18**, 100701 (2015).
[33] C. Emma, A. Lutman, M. W. Guetg, J. Krzy-

winski, A. Marinelli, J. Wu, and C. Pellegrini, Applied Physics Letters **110**, 154101 (2017), http://dx.doi.org/10.1063/1.4980092.

[34] C. Emma, Y. Feng, D. C. Nguyen, A. Ratti, and C. Pellegrini, Phys. Rev. Accel. Beams **20**, 030701 (2017).

[35] J. MacArthur, J. Duris, Z. Huang, and A. Marinelli, in *8th Int. Particle Accelerator Conf.(IPAC'17), Copenhagen, Denmark, 14â 19 May, 2017* (JACOW, Geneva, Switzerland, 2017) pp. 2848–2850.

[36] Y.-C. Chao, *SLAC-PUB-16935, Distributed matching scheme and a flexible deterministic matching algorithm for arbitrary systems*, Tech. Rep. (2017).

[37] W. Qin, Y. Ding, A. A. Lutman, and Y.-C. Chao, Phys. Rev. Accel. Beams **20**, 090701 (2017).

[38] K. Bane and G. Stupakov, Nuclear Instruments and Methods in Physics Research Section A: Accelerators, Spectrometers, Detectors and Associated Equipment **690**, 106 (2012).

[39] J. Zemella, K. Bane, A. Fisher, M. Guetg, Z. Huang, R. Iverson, P. Krejcik, A. Lutman, T. Maxwell, A. Novokhatski, G. Stupakov, Z. Zhang, M. Harrison, and M. Ruelas, Phys. Rev. Accel. Beams **20**, 104403 (2017).

[40] M. Guetg *et al.*, in *Proc. of International Particle Accelerator Conference (IPAC'16), Busan, Korea, May 8-13, 2016*, International Particle Accelerator Conference No. 7 (JACoW, Geneva, Switzerland, 2016) pp. 809–812.

[41] E. Prat, S. Bettoni, and S. Reiche, Nuclear Instruments and Methods in Physics Research Section A: Accelerators, Spectrometers, Detectors and Associated Equipment **865**, 1 (2017), physics and Applications of High Brightness Beams 2016.

[42] M. W. Guetg, *Optimization of FEL performance by dispersion-based beam tilt correction*, Ph.D. thesis, ETH Zurich (2015).

[43] P. Emma, *Beam Stay-Clear Aperture*, Tech. Rep. (LCLSII-2.1-PR-0352, 2015).

[44] V. Kimberg and N. Rohringer, Structural Dynamics **3**, 034101 (2016).

[45] A. Meents *et al.*, Nature Communications **8** (2017), 10.1038/s41467-017-01417-3.

[46] J. Amman *et al.*, Nature Photonics **6**, 693 (2012).

[47] Y. Ding *et al.*, Phys. Rev. Accel. Beams **19**, 100703 (2016).

[48] C. Behrens *et al.*, Nature Communications **5** (2014), 10.1038/ncomms4762.

[49] P. Heimann *et al.*, Review of Scientific Instruments **82**, 093104 (2011), https://doi.org/10.1063/1.3633947.

[50] J. J. Turner *et al.*, Journal of Synchrotron Radiation **22**, 621 (2015).

[51] S. Reiche, Nuclear Instruments and Methods in Physics Research Section A: Accelerators, Spectrometers, Detectors and Associated Equipment **429**, 243 (1999).